Revista de Metalurgia
January-March 2023, 59 (1), e237
ISSN-L: 0034-8570
https://doi.org/10.3989/revmetalm.237

Performance of resistance spot weld caps coated with Ni and Fe aluminide alloys by electro spark deposition on hot dip galvanized steel

İbrahim F. Açış[a], Şükrü Talaş[b,*]

[a] Beyçelik-Gestamp, Inc. Co., Bursa, Turkey
[b] Department of Metallurgical and Materials Engineering, Faculty of Technology, Afyon Kocatepe University, Afyon, Turkey
(*Corresponding author: stalas@aku.edu.tr)

Submitted: 20 December 2022; Accepted: 17 March 2023; Available On-line: 27 April 2023

ABSTRACT: Resistance spot welding (RSW) is widely used as a main joining technique in industry and the electrode caps are frequently replaced because of the degradation during service. In this study, the G type copper RSW electrode caps were coated with Fe and Ni based Fe_3Al, FeAl, Ni_3Al, NiAl alloys by Electro-Spark Deposition (ESD), providing resistance to hot deformation, oxidation and Zn evaporation from sheet metal. The ESD coated electrode caps were tested in-situ on a hot dip galvanized steel in order to assess the performance of RSW electrode caps. For this purpose, three different coating voltages were selected for each coated electrode, and 12 different cap coatings were produced in total. Fifty resistance spot welds were consecutively manufactured with the same parameters for each type of coating electrodes. Hardness measurements, macrostructural examination, Ultrasonic Testing (UT) and chisel tests were performed on welded samples produced. In addition, effects of different coatings on RSW electrode caps were investigated on microstructural development, hardness variations and deformation capacity of resistance spot welds. Results showed that chisel tests and cross section thickness values of the welded sample made with the caps that were ESD coated with the Ni_3Al electrode produced better results than the other caps. The cross-sectional thickness of nuggets was lower in all 158 V coated caps. The performance of aluminide coatings on RSW electrode caps can be listed from the best to the worst in the order of Ni_3Al, NiAl, Fe_3Al, and FeAl.

KEYWORDS: Electro-spark deposition; Hot dip galvanized steel; Iron aluminides; Nickel aluminides; Resistance spot welding

Citation/Citar como: Açış, I.F.; Talaş, S. (2023). "Performance of resistance spot weld caps coated with Ni and Fe aluminide alloys by electro spark deposition on hot dip galvanized steel". *Rev. Metal.* 59(1): e237. https://doi.org/10.3989/revmetalm.237

RESUMEN:*Comportamiento de los tapones de soldadura por resistencia por puntos recubiertos con aleaciones de aluminuros de Ni y Fe mediante deposición por electro-chispa sobre un acero galvanizado en caliente.* La soldadura por resistencia por puntos se utiliza ampliamente como técnica principal de unión en la industria y las capu-

Copyright: © 2023 CSIC. This is an open-access article distributed under the terms of the Creative Commons Attribution 4.0 International (CC BY 4.0) License.

chas de los electrodos se sustituyen con frecuencia debido a su degradación durante el servicio. En este estudio, las capuchas de electrodo RSW de cobre de tipo G se recubrieron con aleaciones de Fe y Ni basadas en Fe_3Al, FeAl, Ni_3Al, NiAl mediante deposición por electro-chispa, proporcionando resistencia a la deformación en caliente, a la oxidación y a la evaporación del Zn de la chapa metálica. Las capuchas de electrodo recubiertas por estas fases intermetálicas se ensayaron in situ sobre un acero galvanizado en caliente con el fin de evaluar su rendimiento. Para ello, se seleccionaron tres voltajes diferentes para cada electrodo recubierto, y se produjeron 12 recubrimientos diferentes en total. Se fabricaron consecutivamente 50 soldaduras por resistencia por puntos con los mismos parámetros para cada tipo de electrodo y revestimiento intemetálico. Se realizaron mediciones de dureza, exámenes microestructurales, pruebas ultrasónicas y pruebas de cincelado en las muestras producidas. Además, se caracterizó la evolución de la microestructura de los diferentes recubrimientos, las variaciones de dureza y la capacidad de deformación de las soldaduras por resistencia por puntos. Los resultados mostraron que los ensayos de cincelado y los valores de espesor de la sección transversal de la muestra soldada realizada con las capuchas de Ni3Al produjeron mejores resultados que las otras capuchas. El espesor de la sección transversal de los electrodos fue menor en todos los casquillos recubiertos utilizando 158 V. El rendimiento de los recubrimientos de aluminuro puede enumerarse, del mejor al peor, en el siguiente orden: Ni_3Al, NiAl, Fe_3Al y FeAl.

PALABRAS CLAVE: Acero galvanizado en caliente; Aluminuros de hierro; Aluminuros de níquel; Deposición por electro-chispa; Soldadura por resistencia eléctrica por puntos.

ORCID ID: İbrahim F. Açış (https://orcid.org/0000-0002-7748-6518); Şükrü Talaş (https://orcid.org/0000-0002-4721-0844)

1. INTRODUCTION

Resistance Spot Welding (RSW) is one of the many joining techniques of mass production and used intensively in the assembly of sheet metals. A constant electrical resistance between spot weld electrode caps and sheet metal should be maintained for retaining the quality of spot welds. RSW electrode caps should have definitive material properties such as high thermal, creep and abrasion resistances, good electrical conductivity, and resistant to mechanical loads depending on their area of use (Aslanlar, 2006; Zhang *et al*., 2008). During welding operations, the exposure to clamping forces at high temperature, high temperature generated by the joule effect causes a bulk deformation of the cap which should be controlled to obtain a predetermined and definite size of the weld nugget (Li *et al*., 2001). Although the RSW electrode cap is chilled by water cooling systems, there is no permanent solution to these deformations. The flattening, chipping, brassing, swelling and wear of the cap surfaces influence the density of the electrical contact resistance against the current to pass, resulting in the formation of poor-quality weld nuggets during the service. The deterioration rate of electrode caps varies depending on the material of the electrode, its form, the welding temperature, heating/cooling rates, and weld clamping forces (Li *et al*., 2001; Williams and Parker, 2004). In order to extend the service life of copper electrode caps, electrode dressing, and sanding processes are applied periodically onto the surfaces. Thus, the service life can be increased by adjusting the topology of contact surface of the copper electrode caps and the electrode dressing frequencies. However, the resistance welding parameters such as welding current, force and welding and holding time can be kept under control, which is also an attractive property when metal sheets are subjected to clamping deformation by electrodes at high temperatures during RSW process (Choi *et al*., 2001; Wan *et al*., 2014). The wear of resistance spot weld electrode caps is mostly the result of thermo-mechanical work that is caused by compression forces and high current passage generated during welding operation. High welding currents or long welding and holding durations accompanied with high clamping forces will cause excessive deformation of sheet metal and/or produce a weak weld strength, over/undersized weld nugget and expulsion process. The wear of electrode caps is accelerated when low melting-point-coating materials are also present on the surface of the steel. The presence of such coatings on the steel causes the surface of the electrode cap alloyed which consequently diminishes their properties such as toughness. In RSW of galvanized steel sheets, the zinc coating evaporates rapidly and cover the surface of electrode caps and forms hard intermetallic compounds on electrode surface, causing Cu electrodes rapidly degrade; similar problems exist with Al-Si coating on the steel, too (Holliday *et al*., 1995; Wan *et al*., 2014).

Intermetallic alloys, such as aluminides, are the type of materials with mechanical and thermal properties between metallic and ceramic materials and have been intensively investigated in recent years owing to their interesting physical and corrosion properties i.e. having better wear and oxidation resistance compared to most metals used at high temperatures. The main disadvantages of intermetallic alloys are their undesirable properties such as low ductility and poor fracture toughness. Recent studies on Ti, Fe and Ni aluminides have focused on brittleness problems which may be eliminated by microstructural variations, grain structures and compositions by keeping the alloying and production processes under control (Tortelli and Natesan, 1998; Judkins and Rao, 2000; Talaş, 2018). Their hardness is quite stable, and their corrosion and wear resistances are better than some of the alloyed and unalloyed metals because of Al_2O_3 film forming on their surfaces. Ni-based intermetallic compounds, i.e. NiAl

and Ni_3Al, are shown as candidate materials for high temperature applications and coating processes against oxidation, as much as Fe based aluminide intermetallic alloys which are more resistant to sulfide rich environment. They are the most stable structures in the Al-Ni system and have the highest melting point, low density, good strength and high temperature corrosion and oxidation resistance (Schaefer *et al*., 1999; Stoloff *et al*., 2000; Talaş, 2018).

Electro Spark Deposition (ESD) creates high frequency micro electric arcs between the electrically conductive (anode) electrode and the base (cathode) material, with a scarce metallurgical effect on the substrate. In the ESD process, the electrode rotation speed, frequency, and voltage/power are controlled. Vibration/axial rotation movement of the electrode is needed to break the electrical current from circuit to the material and the micro welds formed on the surface of the substrate, ensuring constant mass transfer at the micro-level (Parkansky *et al*., 1993; Tang *et al*., 2010; Mertgenç *et al*., 2019). High-current spark between the coating electrode and substrate causes the molten droplets to detach from the anode, provide a perfect adhesion to the cathode substrate and deposits the electrode material on the substrate surface (Tang *et al*., 2010; Gould, 2011; Korkmaz and Ribelko, 2011; Bozkurt *et al*., 2018). The ESD is also applied for purposes such as corrosion, erosion, and wear resistance of materials, reducing or preventing oxidation, reducing the thermal load at high temperatures, reducing maintenance costs etc... (Korkmaz, 2015; Onan *et al*., 2022; Demirbilek *et al*., 2022). Various intermetallic compounds such as FeAl, FeAl+TiC, NiAl and Ni_3Al have been used to coat the surfaces of copper electrode caps to increase the efficiency of RSW using the ESD technique with an elevated wear resistance as much as 3-5 times higher than copper base metal. It is also promising that the number of expulsions and splashes have been drastically reduced after coating with Ni and Al intermetallics. Coatings can be applied to prevent cracking in the electrode. Forming compounds with Zn coating layer on steel sheets may be prevented with the ESD method (Chen and Zou, 2006; Athi *et al*., 2009; Mertgenç *et al*., 2019).

In this study, RSW caps have been coated by the electro spark deposition technique with Ni and Fe based aluminide alloys in order to investigate their effect on wear and mechanical properties of resistance spot welds and caps.

2. MATERIALS AND METHODS

2.1. RSW Caps, intermetallic alloys, and sheet metal

In the experimental study, 13 pairs of copper electrode caps of G type were used, and 12 pairs of the electrode caps were coated with Fe_3Al, FeAl, Ni_3Al and NiAl by the ESD technique, subsequently heat treated and homogenized. Aluminide alloys were selected within the composition range in which the intermetallic structure can easily form and be produced by vacuum arc melting using high purity Ni, Fe and Al powders under the vacuum flushed with Argon gas. Alloy compositions were analysed with EDX (Energy Dispersive X Ray) detector attached to a LEO 1430 VP brand SEM (Scanning Electron Microscope). Coated and uncoated caps were used for RSW of a low strength galvanized 0.75 mm thick DX56D+Z quality steel sheet metal (EN10326 standard) suitable for cold forming. The chemical composition, physical and mechanical properties of the RSW electrode caps and chemical composition of the EN10346 quality sheet metal are given in Table 1 and Table 2, respectively.

2.2. ESD coating process

Twelve G type RSW electrode caps with a tip diameter of 6 mm were divided into 4 groups and manually coated with Fe_3Al, FeAl, $N_{i3}Al$ and NiAl alloy electrodes (rods) in a set of 3 (Fig. 1) under Argon gas. The duration for the ESD coating process was 90 s for each layer and two-layer coating was applied to all RSW electrode caps using the ESD Coating machine (Shanghai Shengzao Mechanical Electrical Equipment Co., Ltd.) Shangai Shengzao SZ03 operating between 40 V to 180 V and 50 Hz to 2.1 kHz. During the coating, electrode rotation speed was 250 rpm for all speci-

Table 1. The chemical composition of the copper welding caps and intermetallic coating electrodes

Welding Electrode	**Copper caps**			
Composition (wt.%)	1% Cr, 0.2 % other, 98.8 % Cu			
Coating Electrodes	Fe_3Al	FeAl	Ni_3Al	NiAl
Composition (at.%)	73% Fe, 27% Al	%53 Fe, %47 Al	%73 Ni, %27 Al	51% Ni, 49% Al

Table 2. Chemical composition of sheet metal (wt. %)

Sheet metal Composition	**C (max.)**	**Mn (max.)**	**P (max.)**	**Si (max.)**	**Al (max.)**	**Ti (max.)**	**Nb (max.)**
EN 10346 DX56D+Z	0.008	0.30	0.025	0.03	0.080	0.15	0.04

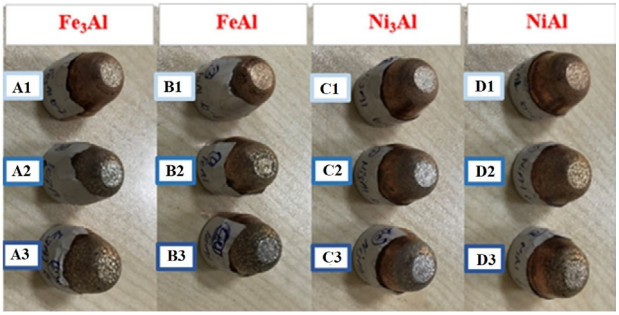

Figure 1. The ESD coated G type copper caps. The first row: 66 V, the second row: 112 V and third row: 158 V. Codes of coating alloys are given above the images.

mens and a constant coating frequency was selected as 1.06 kHz for coating voltages of 66 V, 112 V and 158 V.

2.3. RSW Operations and ultrasonic testing

DX56D+Z quality steel sheet metals were cut in 40x25 cm^2 dimension, and 13+13 sheets were lap joined by RSW (Fig. 2a). In order to prevent parallel current circuits between the plates, equal zones of 20 cm^2 and ~3.5 - 4 cm distances were kept between the resistance spot welds as shown in Fig. 2b, and 50 welds were made with each RSW cap. For the non-destructive testing, an ultrasonic inspection test equipment (USLT-USB, GE Sensing and Inspection Technologies, GmbH, Germany) operating at 20 MHz was used with 3.6 mm probe size designed for ultrasonic testing (UT) of welded samples. The non-destructive UT was applied to the 25th resistance spot of each of the welded plates. Resistance spot weld nugget signals and weld nugget deformation were analyzed on welded plates. Yaskawa model industrial robot was used for RSW operations; 600 (12x50) spot welds were made on 13 different plates at constant welding and holding duration (both are ~0,7 s) under 2200 daN jaw pressure using 6.5 kA current, with electrode temperature between 17-22 ºC, assisted by water circulation. Welding current and (electrode) jaw pressure is a standard procedure for this type of steel and thickness determined by the factory processing route.

2.4. Microstructure, hardness, ultrasonic examinations and chisel tests

The 10th, 20th, 30th, 40th and 50th resistance spot sections of the welded plates were cut with SiC cutting discs as to reveal just the middle section, passed through 320, 600, 800, 1000G grinding stages and polished with a 1 µm alumina suspension. Specimens were then etched with 2% Nital and the microstructure was examined. Metallographic and microstructural analyses were made from the 30th samples taken from the assembly. Photographs were taken from spot welds with Nikon optical microscope and using LEO 1430 VP brand SEM. Microhardness measurements were made using Shimadzu HMV2 microhardness tester on the 1st, 10th, 20th, 30th, 40th and 50th spot welds, using 100 g load, by making 3 indents on the weld nugget of RSW and averages of results are calculated and presented. The welding electrode cap surface was visually and microstructurally examined after the coating and RSW processes. The 41st corner spot welds on each plate, as shown in Fig. 2b, were torn open with the chisel test and then nugget formations and their topology were examined for their appearance to find out the rupture mode of spot welds.

3. RESULTS AND DISCUSSION

3.1. Microstructural analysis and microhardness results of resistance spot welds of uncoated electrode cap

The microstructure of the 30th welded sample made by uncoated cap is shown in Fig. 3a. In the weld microstructure, a weld nugget with borders is observed and a columnar formation of grains is clearly visible around the weld nugget which is decorated with a finer grain structure. In addition, the nugget does not reveal any transverse interface separation line. However, both ends of the nuggets are separated up to the nugget zone and the columnar structure formation indicates that partial melting of the sheet took place and aligned alongside of the heat transfer direction from the nugget towards the base metal (Kaiser *et al.*, 1982; Aslanlar, 2006; Harlin *et al.*, 2003). There is a grain refinement inside the nug-

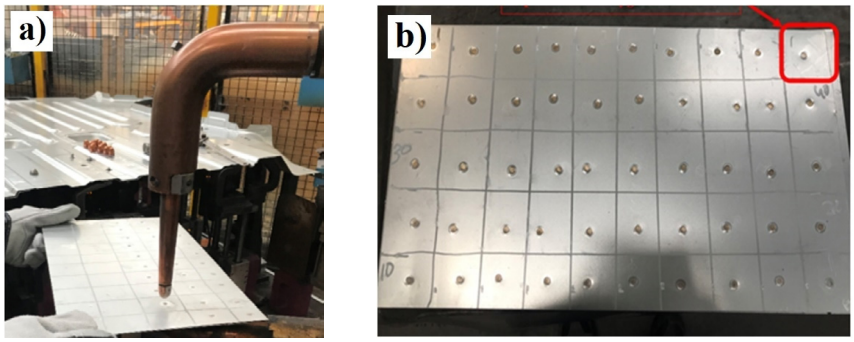

Figure 2. a) The RSW operation b) the resistance spot welded plates indicating the tearing test location.

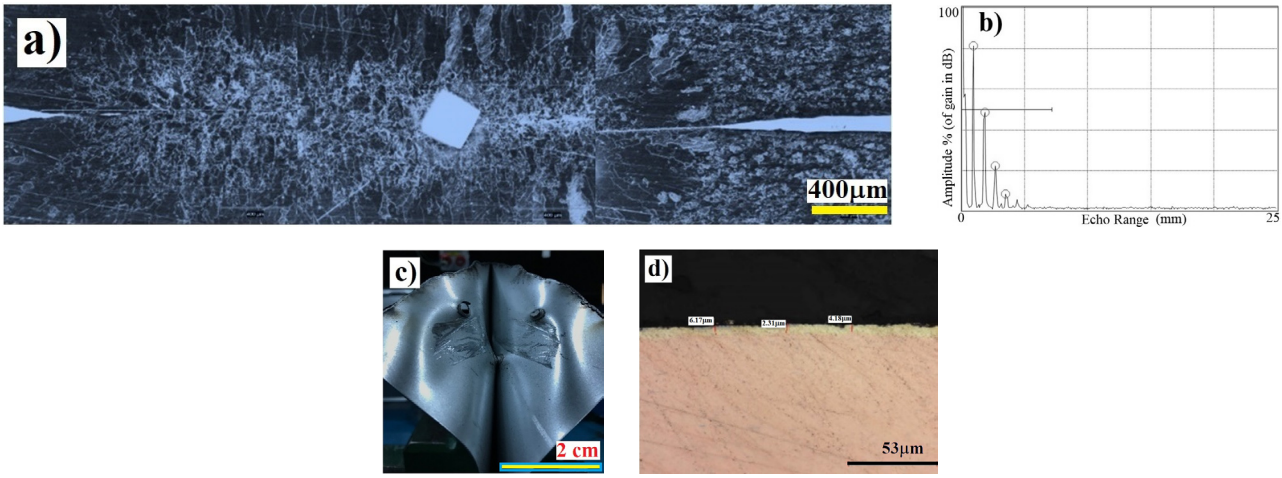

Figure 3. a) Microstructural image of the resistance spot welds made by uncoated electrode caps; b) ultrasonic test plots of spot welds made by uncoated copper electrode caps (horizontal line shows the threshold of 1.05 mm thickness of the spot weld zone; amplitude is given in the x axis and the distance is given in the y axis, c) destructive test result of resistance spot weld by uncoated cap, d) post weld microstructure of the cap without coating (avrg. 5.69 µm thick Zn rich layer).

get of the weldment, which may be either due to fast cooling of weld zone heated by joule effect. The electrical current runs for a short time during which sheets of metal fuse together, but the electrodes continue applying pressure and the cooling rate of the electrodes affects the weld metal solidification mode. As the resistance forms at the interface between two sheets of metal, heat is evolved from the joint as the current is applied, however, melting, and consequent solidification of the resistance spot weld forces the initial solidification front to undergo the formation of the columnar grain structure as the current is no longer available. The edges of the weld zone transform from a near-delta ferrite structure and cools faster just after the current is cut off, forming a heat affected zone (HAZ) of coarse and then fine grain structures (Song *et al.*, 2005; Rogeon *et al.*, 2008; Luo *et al.*, 2016). The thickness of Zn rich layer formed on the uncoated cap due to the Zn coating on steel is around 6 µm (Fig. 3d) and no microcracks were observed in this layer. As it is seen in Fig. 4, a Zn rich layer is present and its thickness is around 35 µm. The melting point of Zn is relatively lower than that of the steel and Zn evaporates because of the heating by resistance and is accumulated on the surface of Cu electrode, which is cooled by water circulation. As with time and heat, the Zn diffusion to the Cu electrode base is accelerated and a Zn rich layer of high resistance is formed on the surface of the Cu electrode, which usually requires slightly more current to spike up the temperature of the nugget of RSW in addition to the intrinsic increase of the electrical resistance due to high temperature. A sudden melting and/or a high temperature due to the joule heating are the reasons for the accelerated diffusion at the interface of the Zn coated steel and Cu electrode cap. It appears to be a gradual thermo-diffusion driven change in the amount of Zn as it progresses towards the inner part from Cu cap surface. The alloying effect of the Zn on the Cu electrode is a well known phenomena and the coating electrode surface with TiC, TiB_2 and some intermetallics help preventing the diffusion of the Zn and hardening of the surface layer (Tang *et al.*, 2010; Mertgenç *et al.*, 2019). This layer dominantly affects the hardness of surface of the Cu electrode cap after RSW is carried out at many times. As it can be seen in Table 3, the average of

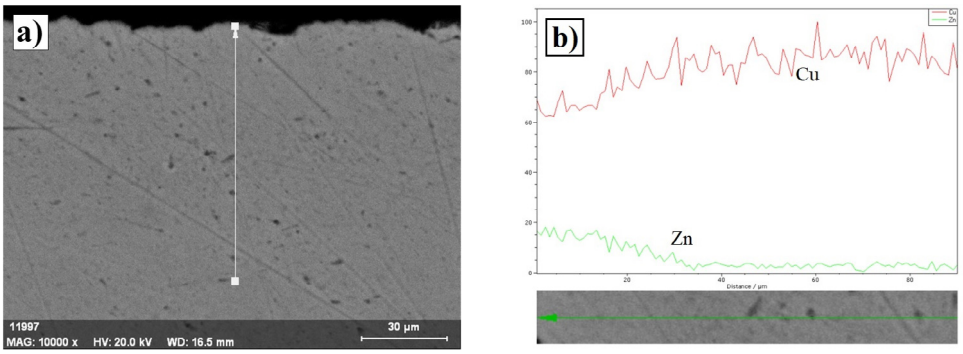

Figure 4. An SEM image from the cross-section surface of the uncoated electrode and a line scan after 50 cycles showing Zn variations in the Cu electrode.

Table 3. Hardness measurement values of uncoated copper electrode surface after 50 RSW operations

Hardness (HV)					
Uncoated					
0.	10.	20.	30.	40.	50.
102	133.6	149.0	149.6	156.4	160.1

the hardness values of the RSW electrode caps after 50 welding operations is 160.1 HV, which is higher than the uncoated Cu matrix hardness (102 HV). As the number of RSW increases, the surface hardness of copper caps also increases as a result of both the thermomechanical work that hardens the matrix and the effect of alloying with Zn coating on the steel sheet as shown in Fig. 4.

Ultrasonic Test Results of Resistance Spot Welds by Uncoated Electrode Cap

The UT signals of the welded sample obtained by the uncoated cap are shown in Fig. 3b. It has been determined that the signals are logarithmic, noiseless and a homogeneous core is formed in the test graph, where the signal intensity is observed to be usual. In the experiments with samples having a lower threshold tolerance of 1.05 mm thickness, the resistance spot weld thickness was measured to be 1.23 mm in the welded sample made with the uncoated electrode cap. This is an average value for most of the welded samples which are accepted as a "pass" by the manufacturer.

Chisel Test Results of Resistance Spot Welds of Uncoated Electrode Caps

The post-weld chisel test of the welded sample made with the uncoated cap is given in Fig. 3c. The nugget core is nicely formed and the chisel damage at the edge of both facing sides of the metal sheets reveals that there was sufficient joining along the weld nugget. The face of electrode cap is given in Fig. 3d and a layer with an average thickness of 5.69 µm is visible, which is possibly an indication of brassing due to Zn evaporation during the spot welding. It is brittle and reduces the life of electrode caps by chipping of edges and forming large cracks extending to the unaffected part of the electrode caps (Harlin *et al.*, 2003; Chen and Zhou, 2006).

3.2. ESD coated electrode caps

Microhardness Results

In the hardness tests performed on the 10th, 20th, 30th, 40th and 50th samples cut from the plates. The most noticeable variation in hardness occurred in the caps coated with the Fe_3Al intermetallic alloy. As in Table 4, it has been determined that the welded sample joined with Fe_3Al coated caps with the coating voltages of 66 V and 112 V are harder than the others. The plate that shows the largest variability among their hardness is the one welded with the cap coated with Ni_3Al at 158 V. A sharp hardness difference of 13.1 $HV_{0.1}$ was observed between the 10th weld and the 30th weld. Plates with the lowest hardness deviation were determined as those welded with the Ni_3Al and NiAl coated caps at 112 V. Although a metallurgical alloying is present between the coating and the substrate (Korkmaz, 2015; Onan *et al.*, 2022), having a distinct elasticity modulus between them is a very challenging situation. During the course of applying pressure and being exposed to heat from the lap joint accelerate the wear process of coating and Cu caps with a secondary effect from deformation of copper caps. After certain number of pressing during RSW, in addition

Table 4. Hardness values of resistance spot weld nuggets with respect to coating voltage and type of coating

Electrode Alloy	Fe_3Al					FeAl					Ni_3Al					NiAl				
Weld number	10.	20.	30.	40.	50.	10.	20.	30.	40.	50.	10.	20.	30.	40.	50.	10.	20.	30.	40.	50.
66V	201.1	202.6	202.6	208.5	210.5	199.0	196.2	206.4	202.4	197.7	197.3	198.1	203.4	199.0	199.2	200.9	203.4	198.2	197.0	192.7
	205.1 HV					200.3 HV					199.4 HV					198.4 HV				
112V	214.9	216.7	211.5	211.4	207.2	202.2	200.1	198.0	195.8	200.6	198.5	202.3	199.9	201.8	198.4	199.8	203.7	201.1	199.6	198.1
	212.3 HV					199.3 HV					200.2 HV					200.5 HV				
158V	199.7	202.0	200.4	198.6	199.4	199.8	198.5	196.3	199.4	194.8	195.3	197.9	198.4	205.0	202.1	202.4	197.7	200.4	202.2	196.5
	200.0 HV					197.8 HV					201.7 HV					199.8 HV				

to the zinc accumulating on the surface, nugget hardness is expected to show variation as it is seen in Table 4. The variation in hardness in the series is not profoundly distinctive but a gradual change in some series is still observable. Apart from small changes, they are all within the similarity range of 200 HV. These results are lower than the bulk Fe_3Al, FeAl, Ni_3Al and NiAl aluminide intermetallic alloys' hardness values, which is possibly due to the layer effect i.e. alloying with the substrate and low thickness of the aluminide coatings. Within the voltage series, changes are again not profound. In terms of type of electrodes, the aluminide intermetallics having ordered phases of bcc B2 superstructure (NiAl and FeAl) are expected to have a higher hardness due to their increased brittleness as a result of a lower number of slip planes that are activated during the plastic deformation compared to A_3B type of intermetallics, i.e. Fe_3Al ($D0_3$ superstructure, bcc) and Ni_3Al ($L1_2$ superstructure, fcc). It is also possible that the increased hardness of B2 superstructures is due to the thermal vacancies occurring after the high temperature treatment and antisite vacancy formation and fast cooling rate (Morris and Munoz-Morris, 2005; Krein *et al.*, 2007). However, such defects may result in an easy glide of dislocation planes at high temperature but not at low temperatures. Assuming that such defects were retained until room temperature due to having a sufficiently high cooling rate, the hardness is believed to be well affected by such defects (Schaefer *et al.*, 1999; Terada *et al.*, 2002).

Ultrasonic Test Results and Post Weld Coating Microstructures

The interpretation of the ultrasonic test (UT) graphics obtained from the RSW specimens is given in Fig. 5. All contact surface echoes that exceed 80% were measured for all weld nuggets. Ni_3Al/66 V, Ni_3Al/112 V, NiAl/66 V and Fe_3Al/66 V spot welds were found to be the most homogenized weld nuggets, showing logarithmic and noiseless reduction, respectively. The worst performance was from FeAl/158 V RSWs. The deformations, in terms of RSW thickness detected because of the UT tests, are plotted in Fig. 6. If the threshold limit is set below 30% as a risk percentage and set it as 1.05 mm for the combined total thickness of 1.5 mm, all welded samples made with electrode coated with 66 V are suitable for pass mark, while only those coated with Ni-based aluminide

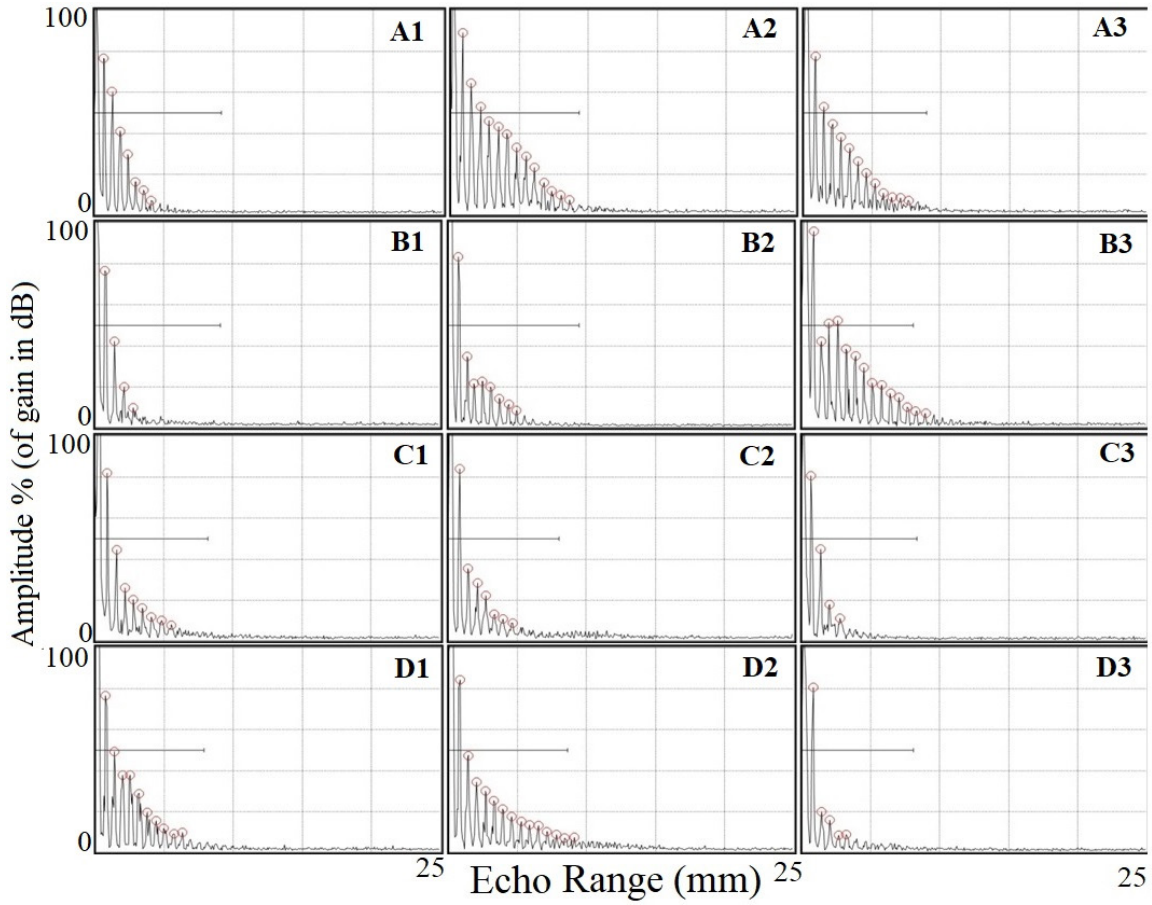

Figure 5. UT plots of resistance spot welds made with the Fe_3Al coated caps (A1) 66 V, (A2) 112 V and (A3) 158 V; the FeAl coated cap (B1) 66 V, (B2) 112 V, (B3) 158 V; the Ni_3Al coated cap (C1) 66 V, (C2) 112 V and (C3) 158 V; the NiAl coated cap (D1) 66 V, (D2) 112 V and (D3) 158 V. The horizontal line in the images shows the threshold of 1.05 mm thickness of the spot weld zone.

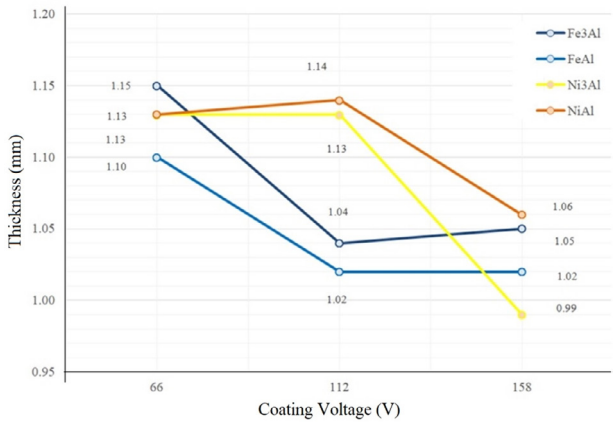

Figure 6. The weld nugget cross section thickness values against the coating voltages.

intermetallics at 112 V can be considered suitable for the ESD coating condition; however, the performance of the coatings may differ in practice, hence, it should be tested in situ. The most striking finding is that the coating voltages have a direct effect on the RSW deformation, with respect to the type of coating electrode material, and the type of electrode has a profound effect on the nugget cross section thickness of RSW. Figure 6 shows that the lowest cross section thickness is obtained with FeAl and Fe_3Al with the exception of Ni_3Al at the coating voltage of 158 V. This behaviour may be related to the thermal conductivity of the coating. The thermal conductivity of NiAl is approximately 80 W/mK while it is less than 25 W/mK for the Ni_3Al alloys. The thermal conductivity of the Fe_3Al is lower than that of the FeAl, which is lower than that of the NiAl and the Ni_3Al (Athi *et al.*, 2009). Hence, the coatings with Fe aluminides have lower thermal conductivity than the Ni aluminides. This would affect the heat transfer from the weld zone and create a barrier for heat flow towards the cooled electrode caps (Bozkurt *et al.*, 2016). Figure 6 show that the low thermal conductivity of the Fe aluminides produces a lower cross-sectional thickness for 112 V and 158 V coatings except for the NiAl and the Ni_3Al (for 158 V is lower). For the Ni_3Al-158 V case it is obvious that the thickness of the coating was greater than the rest of the coatings. This results in a low heat conductivity from the heat generating interface, i.e. lap joint, towards the RSW caps and, hence, causes the accumulation of heat at the nugget zone, increasing the heat in the weld region and making it more plastically easy to deform. Similar mechanisms are valid for the low thermal conductivity alloys, i.e. Fe aluminides, as it is shown in Fig. 6. The best performance is observed with NiAl, which has the highest thermal conductivity amongst the aluminide type intermetallic alloys studied in this work.

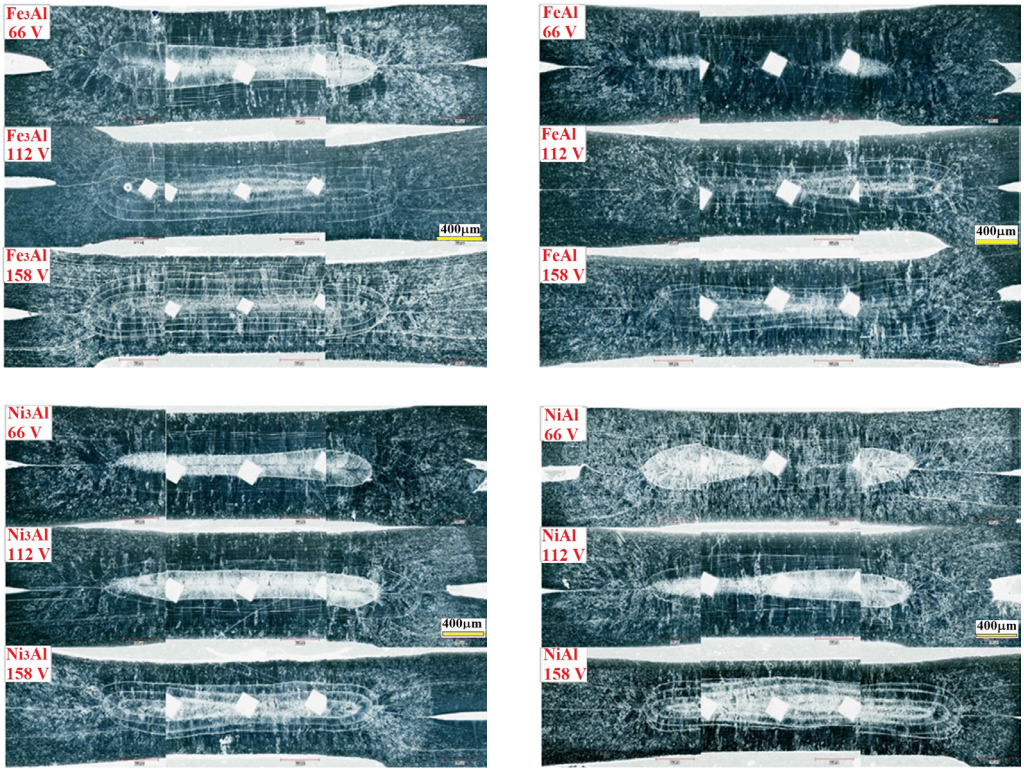

Figure 7. Macrostructure images of the weld nuggets made with the Fe_3Al, the FeAl, the Ni_3Al and the NiAl coated caps. Coating voltages and codes are given in each image.

Macrostructural and microstructural analysis of resistance spot welds by coated caps

The cross-sectional images of the 30th RSWs are shown in Fig. 7. A clear nugget structure was observed in welded samples made with the Fe_3Al/66 V, the Ni_3Al/66 V, the Ni_3Al/112 V and moderately with the NiAl/112 V and the NiAl/66 V caps. Among them, the most homogeneous one was observed in the RSW with the Ni_3Al/112 V. Microstructural examinations of the Fe_3Al/112 V, the Fe_3Al/158 V, the FeAl/112 V, the FeAl/158 V, the Ni_3Al/158 V and the NiAl/158 V showed that excessive nugget deformations were observed within the melting zone extending to the surface.

The microstructures of the coated caps taken at 100x magnification from the cross-section are shown in Fig. 8. The average values of the coating thicknesses ob-

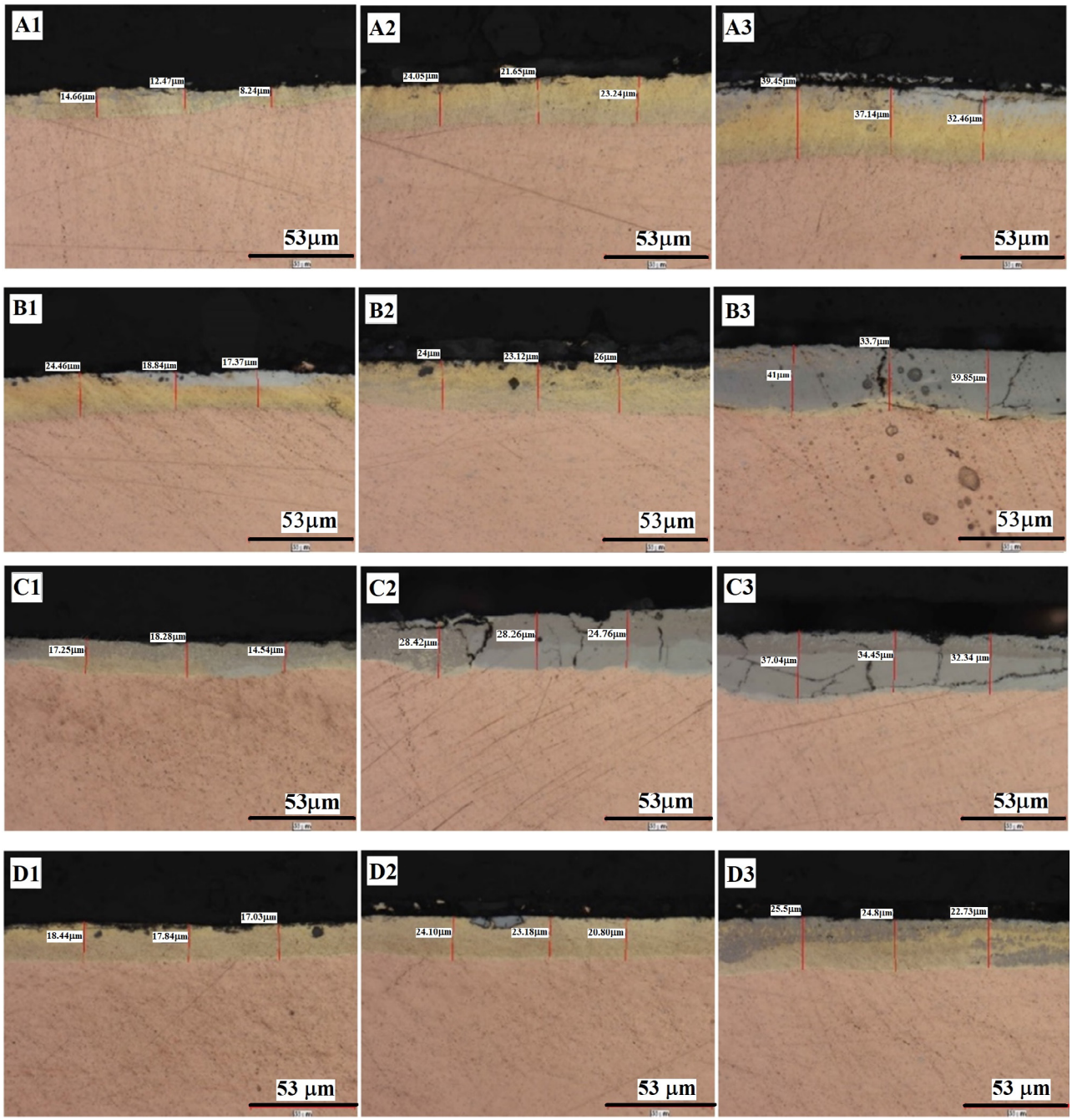

Figure 8. Post weld coating microstructures of row A; the Fe_3Al coated caps. 1) 66 V, 2) 112 V, 3) 158 V, row B: the FeAl coated caps 1) 66 V, 2) 112 V, 3) 158 V, row C: the Ni_3Al coated caps 1) 66 V, 2) 112 V, 3) 158 V, row D: the NiAl coated caps 1) 66 V, 2) 112 V, 3) 158 V. Scale bar is 53 µm.

tained from the optical images were analyzed and given in Fig. 9. In addition, the coating topologies were examined and the differences between the coatings were compared. All coated electrodes show a good metallurgical bonding with the copper base metal and mostly homogeneous and continuous line of coating is present along the coating layer. The phase transformation points of these aluminide intermetallics alloys are important in their behaviour. Intermetallics have order-disorder transformation points of 1310 ºC for the FeAl, 552 ºC for the Fe_3Al, 1300 ºC for the Ni_3Al and 1630 ºC for the NiAl alloy (Schaefer *et al.*, 1999; Krein *et al.*, 2007). Most intermetallics are profoundly stable in their properties below their order-disorder transition temperature and, hence, high hardness and high elasticity module are common for such alloys at low temperatures, in this respect, the temperatures around 200 ºC at the electrodes are not greatly high to defer their properties, however, at the contact point the temperatures are very high and the properties of the intermetallic layers are not preserved on cooling (Mikno and Bartnik, 2016). However, long heat treatment regimes are needed to obtain fully intermetallics structures, fast cooling of coating layer just after RSW may not be sufficient to conserve such properties. This may not be valid in the NiAl system because of its high order-disorder temperature but the rest of the intermetallic coatings are not fully functional in ordered state unless the cooling medium is sufficiently effective in reducing the interface temperature. Figures 8 and 9 show that because the post weld thickness of the Ni_3Al intermetallic layer on copper cap is relatively high, this may have caused an increase in interface resistance and temperature. Such an increase in the interface temperature would increase the plasticity of the metal sheets being joined, reducing the thickness of lap joint by the deformation. The examination of the coatings on copper caps shows that the coating thicknesses obtained with high voltages are usually higher than the other coating voltages. Among the caps coated with 66 V, the most different topology was observed in the Ni_3Al, while the highest value of the coating layer was measured in the

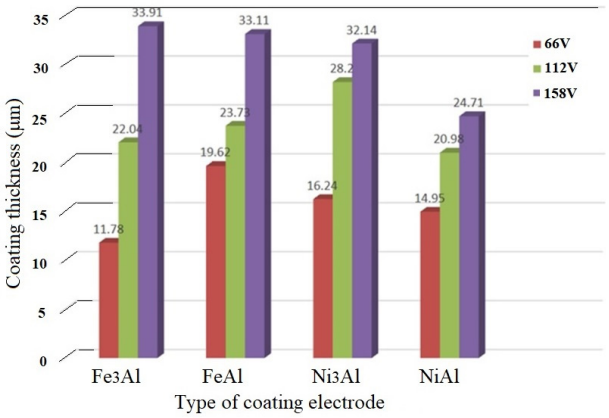

Figure 9. Copper electrode cap coating thickness distribution after the welding process.

FeAl/66 V. Among the caps coated with 112 V, the most different topology was also seen in the Ni_3Al, and scattering in thickness and microcracks were observed in the coating layer. The highest coverage was also measured in the Ni_3Al. Material loss and microcracks were observed in the FeAl and the Ni_3Al between the caps coated with 158 V. Except for the NiAl, coating thicknesses were measured at similar levels for other coatings. The most stable coating increase was observed in the Fe_3Al and the NiAl coatings, and no irregularities were observed in these two coatings in terms of coating behaviour and topology. As it is seen in Fig. 10, Zn appears to have diffused across the coating into the matrix in most electrodes, even though the coating layer is formed by the accumulation of micro droplets unlike of such as powder metallurgy products (Biliz *et al.*, 2020). The Fe aluminide coatings are less effective with preventing Zn diffusion into the coating first and then the Cu matrix. However, the Ni based coatings are more effective in such a way that Zn diffusion as much as Ni has been observed in the Ni_3Al series. It can be noted that the Ni_3Al is more resistant to Zn diffusion from the surface through the coating layer because the Zn line scan does not penetrate to the matrix as did in the NiAl and the Fe-Al series. This would in practice increase the life span of the Cu electrode which is prone to cracking and erosion by Zn diffusion from the Zn coated steels (Bhattacharya, 2018). In the NiAl series, Zn diffusion is similar to FeAl and Fe_3Al series, suggesting that Al content may be related to the diffusion capacity of Zn in the Cu matrix. The material loss from the surface is more pronounced in the FeAl/112 V, the FeAl/158 V series and the Fe_3Al/158 V specimen. There are more cavities in the FeAl/112 V and FeAl/158 V which may be a result of the high temperature corrosion and the Zn-rich phase erosion due to compaction pressure active upon the coating layer during the RSW operation. It is noted that the Fe based intermetallic aluminide alloys are in general more resistant to sulfidation than oxidation at high temperatures compared to the Ni based intermetallic aluminide alloys (Talaş, 2018). Different thermal properties such as the thermal expansion capacities of matrix and the coating layer also play an important role in the formation of cracks and cavities. The ESD coating layer is formed differently such that the ESD deposition is layered, and each micro arc is practically formed in a manner of brick lying. This would pose a problem when the dynamic forces are in question since the layers do not behave as a bulk metal, acting as either soft or very hard region with a weak interface compared to bulk metals. Such weakness can be seen as a source of degradation leading to cavities and fall-outs as shown in Fig. 10, that is, the NiAl 158 V series. As it is seen in the NiAl and the Ni_3Al series (Fig. 10), there is also a tension crack between the matrix and the coating, which may be due to the differences in the thermal properties of the coating interface components. The coefficient of thermal expansion values for the FeAl and the Fe_3Al

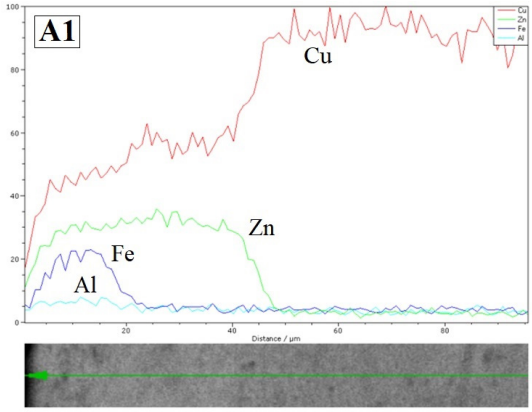
A1
Cu
Zn
Fe
Al
Distance / µm

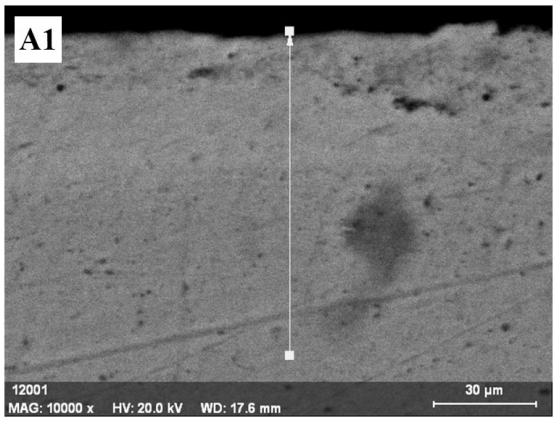
A1
12001
MAG: 10000 x HV: 20.0 kV WD: 17.6 mm
30 µm

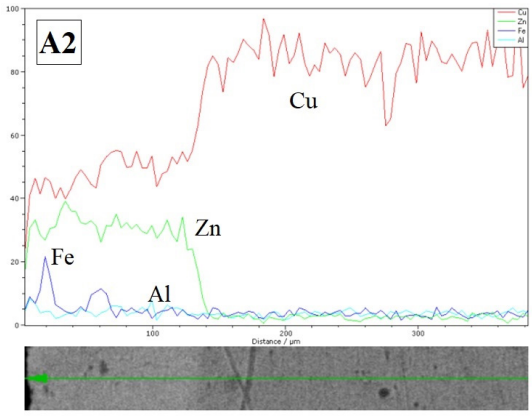
A2
Cu
Zn
Fe
Al
Distance / µm

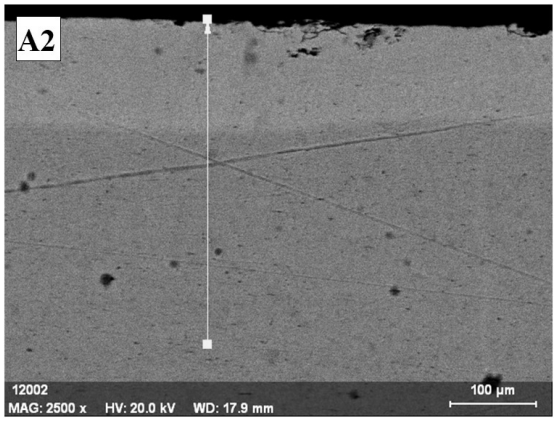
A2
12002
MAG: 2500 x HV: 20.0 kV WD: 17.9 mm
100 µm

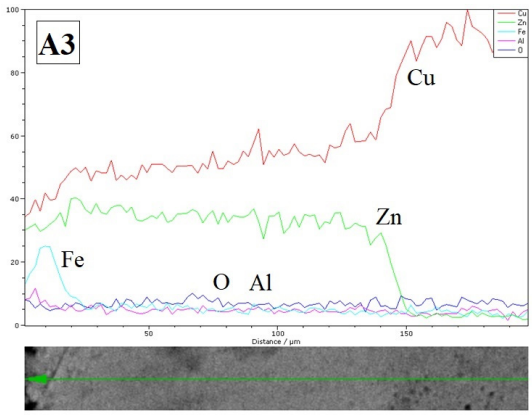
A3
Cu
Zn
Fe
O Al
Distance / µm

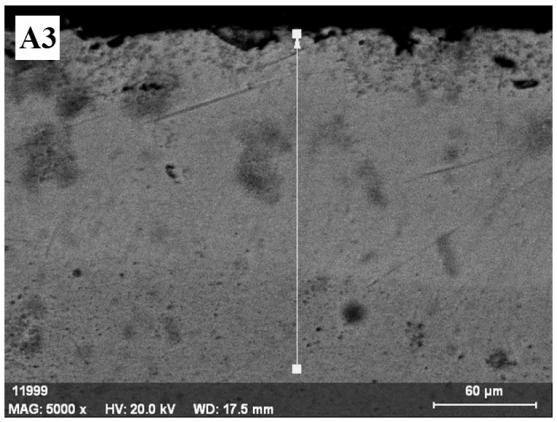
A3
11999
MAG: 5000 x HV: 20.0 kV WD: 17.5 mm
60 µm

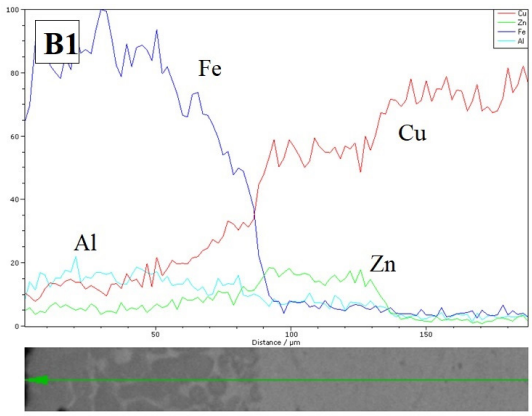
B1
Fe
Cu
Al
Zn
Distance / µm

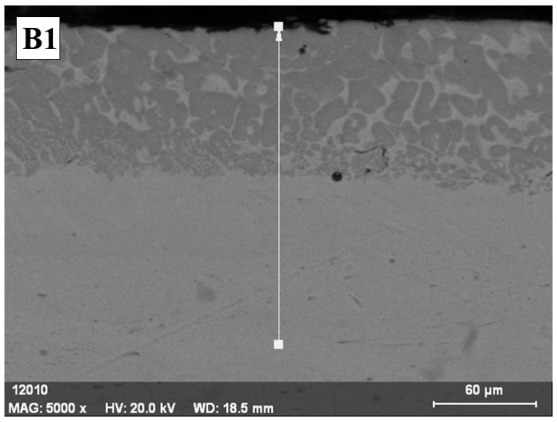
B1
12010
MAG: 5000 x HV: 20.0 kV WD: 18.5 mm
60 µm

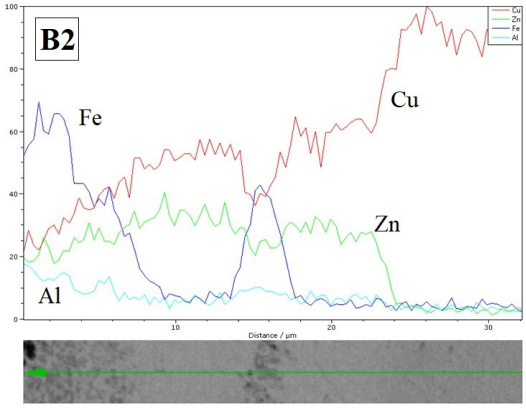
B2
Fe
Cu
Zn
Al
Distance / µm

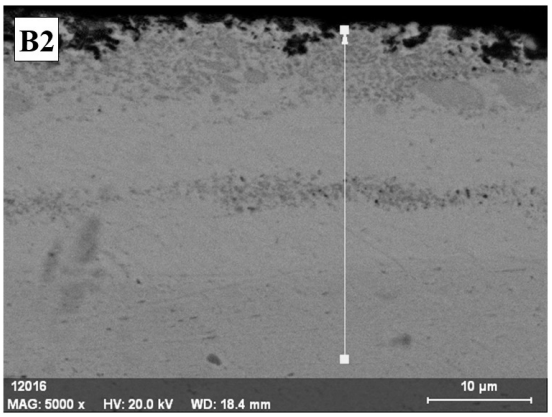
B2
12016
MAG: 5000 x HV: 20.0 kV WD: 18.4 mm
10 µm

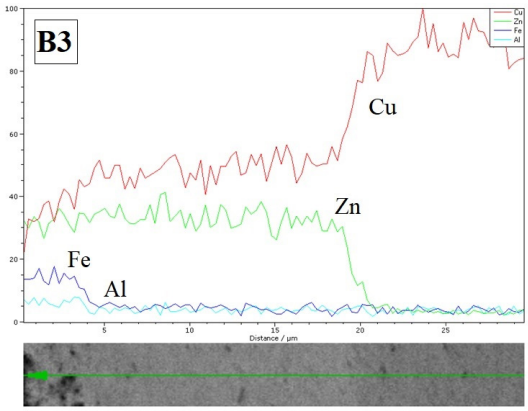
B3
Cu
Zn
Fe
Al
Distance / µm

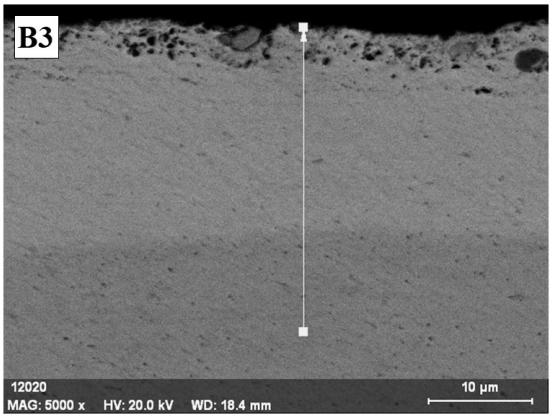
B3
12020
MAG: 5000 x HV: 20.0 kV WD: 18.4 mm
10 µm

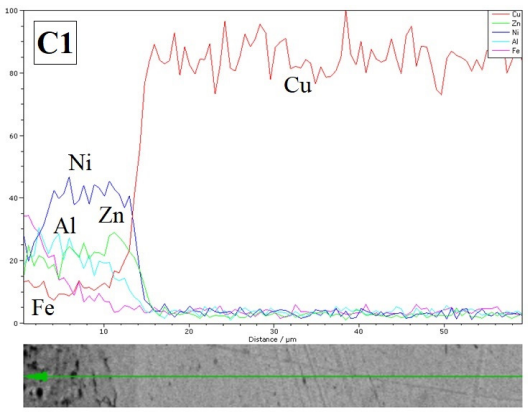
C1
Cu
Ni
Al
Zn
Fe
Distance / µm

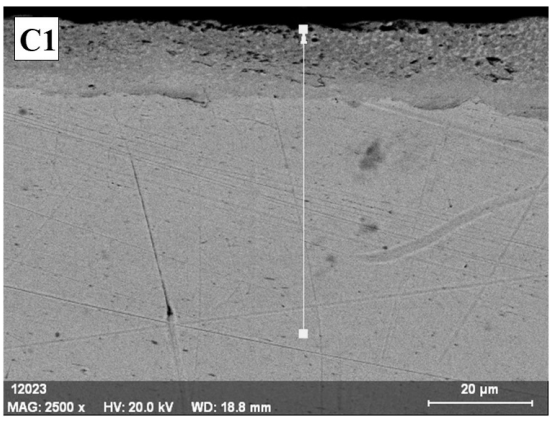
C1
12023
MAG: 2500 x HV: 20.0 kV WD: 18.8 mm
20 µm

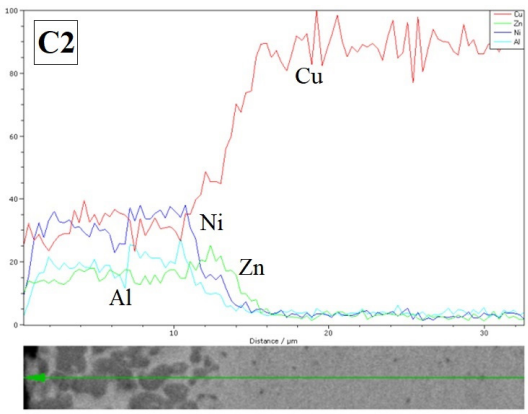
C2
Cu
Ni
Zn
Al
Distance / µm

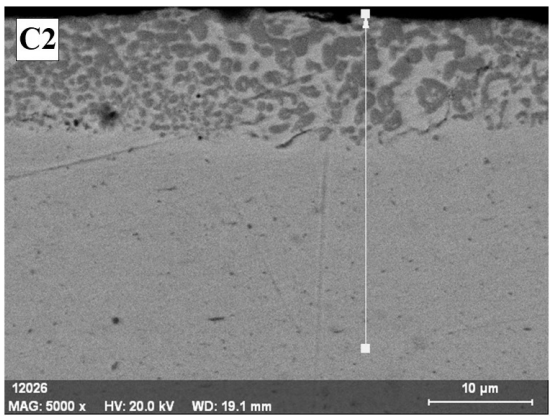
C2
12026
MAG: 5000 x HV: 20.0 kV WD: 19.1 mm
10 µm

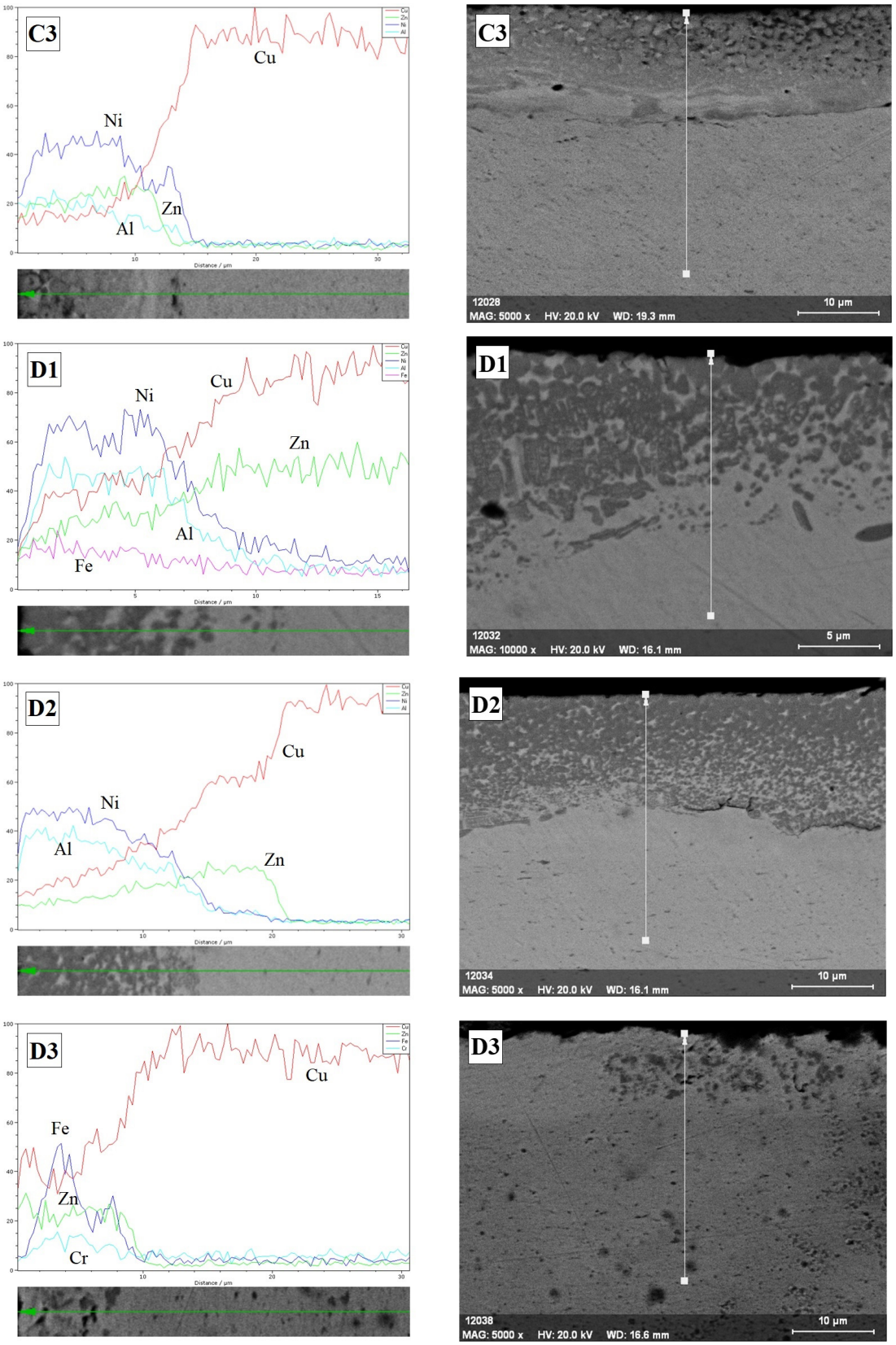

Figure 10. Cross sectional image and corresponding EDX line analysis results of the Fe_3Al (A1 - A3), the FeAl (B1 - B3), the Ni_3Al (C1 - C3) and the NiAl (D1 - D3) from top to the bottom; for 66 V (1), 112 V (2) and 158 V (3) coating voltages, respectively.

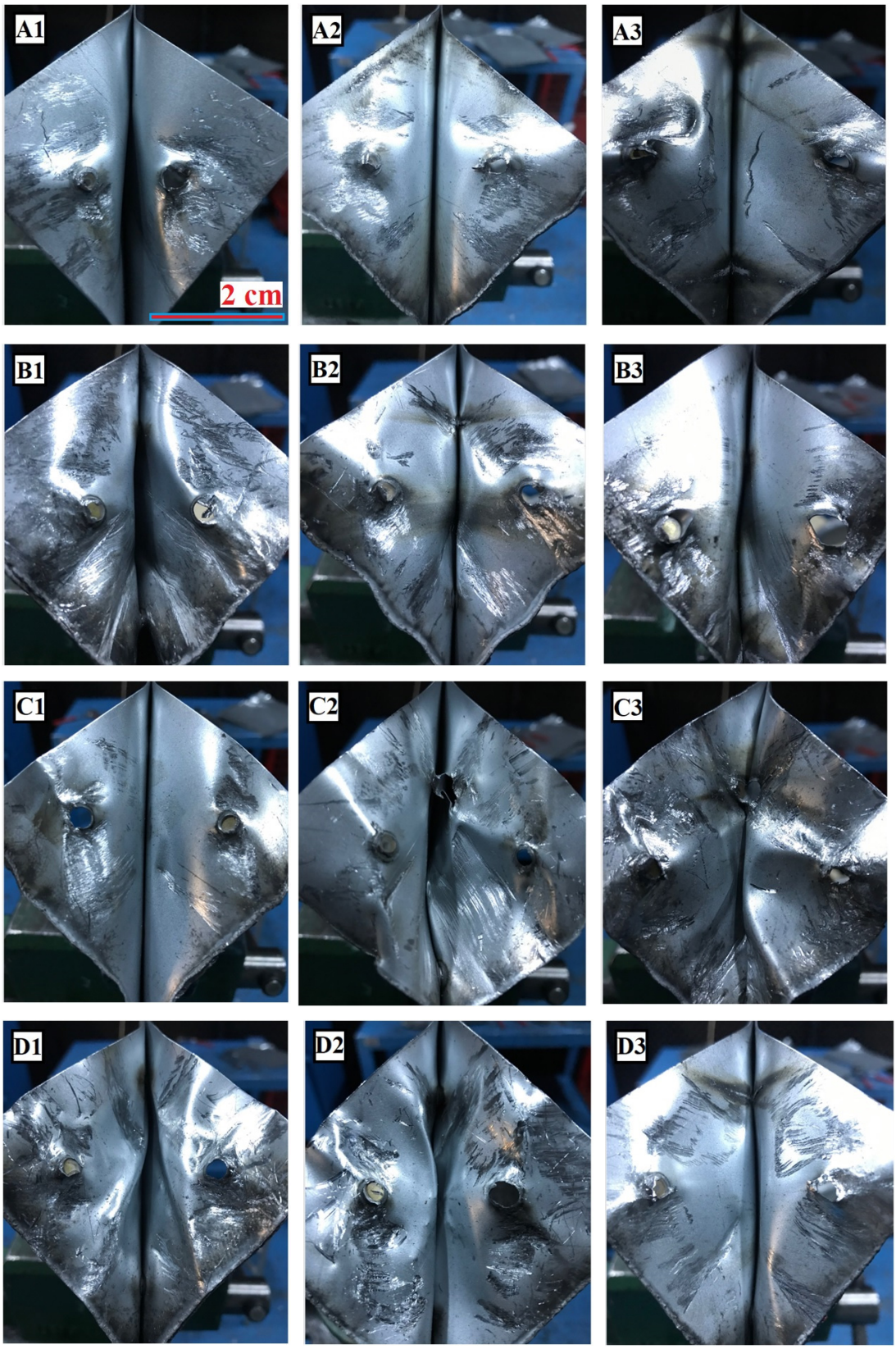

Figure 11. Chisel test results of the resistance spot welds made with, row A; the Fe_3Al coated caps. 1) 66 V, 2) 112 V, 3) 158 V, row B: the FeAl coated caps 1) 66 V, 2) 112 V, 3) 158 V, row C: the Ni_3Al coated caps 1) 66 V, 2) 112 V, 3) 158 V, row D: the NiAl coated caps 1) 66 V, 2) 112 V, 3) 158 V.

are $19.5x10^{-6}$ K^{-1} and $25x10^{-6}$ K^{-1}, while the coefficient of thermal expansion values are $23.5x10^{-6}$ K^{-1} for Cu, $18x10^{-6}$ K^{-1} for Ni, $15x10^{-6}$ K^{-1} for NiAl and $19x10^{-6}$ K^{-1} for Ni_3Al (Wang and Reeber, 1996; Wang *et al.*, 2004; Masset *et al.*, 2009; Švec *et al.*, 2013). It is likely that Cu-NiAl combinations are more prone to contraction stresses during the RSW process with fast heating and cooling conditions.

Chisel Test Results of Resistance Spot Welds of Coated Electrode Caps

Figure 11 shows the specimens after the destructive tests. The RSW nuggets with high rupture resistance were observed for the Ni_3Al/66 V, the Ni_3Al/112 V, the NiAl/66 V, and the NiAl/112 V, respectively. The Ni_3Al/158 V and the NiAl/158 V RSWs broke off more easily in a shear mode compared to the 66 V and the 112 V. The ruptures in the welded sample occurred with the formation of tearing at the edges of the RSW nugget, showing some ductility. It was observed that the RSW nuggets joined with the FeAl coated caps were also smaller in size, supporting the UT test. In the Fe_3Al tests, the RSW made with the 112 V and the 158 V coated caps resulted in premature rupture with an appearance that the borders of the nuggets were not clearly defined. The thickness of the coating in the 158 V series implies that, as the thickness of the coating increases, the joule effect due to the heating by electric current is less effective in producing sufficient heat at the interface of two mating sheet metals, leading to the insufficient formation of the weld nugget core and, hence, a premature failure.

4. CONCLUSIONS

The results from this study can be summarized as follows:

- The Ni-based aluminide alloys produce better spot welds than the Fe based aluminide alloys coated caps based on the appearance of ruptured spot welds after the chisel test and the penetration values of Zn on spot weld caps.
- The Zn diffuses into coating regardless of the type of coating; however, the Ni based coatings are more resistant to the diffusion of Zn towards the copper electrode matrix.
- The coatings help increasing the nugget core hardness compared to the weldments with uncoated electrodes.
- As the intensity of the coating voltage is increased, the coating thickness and the amount of deformation of spot welds also increase as a result of high interface electrical resistance, which causes an increase of the interface temperature and the accumulation of the heat in the nugget of spot welds.
- Increasing the coating voltage levels showed that the post-weld coating microcracks increased, as this is related to the thickness of the coating and, hence, to the interface resistance between electrode and sheet metal.
- The effects of type of aluminide alloy electrodes on the RSW quality can be listed as: Ni_3Al, NiAl, Fe_3Al, FeAl from the best to the worst.

REFERENCES

Aslanlar, S. (2006). The effect of nucleus size on mechanical properties in electrical Resistance Spot Welding of sheets used in automotive industry. *Mater. Des.* 27, 125–131. https://dx.doi.org/10.1016/j.matdes.2004.09.025.

Athi, N., Cullen, J.D., Al-Jader, M., Wylie, S.R., Al-Shamma'a, AI., Shaw, A., Hyde, M. (2009). Experimental and theoretical investigations to the effects of zinc coatings and splash on electrode cap wear. *Measurement* 42, 944-953. https://doi.org/10.1016/j.measurement.2009.02.001.

Bhattacharya, D. (2018). Liquid metal embrittlement during resistant spot welding of Zn-coated high-strength steels. *Mater. Sci. Technol.* 34 (15), 1809-1829. https://doi.org/10.1080/02670836.2018.1461595.

Biliz, İ., Bakkaloglu, A., Kilic, M. (2020). The effect of process parameters on microstructure and porosity of layered NiAl(Co/Cr) alloy produced by SHS method. *J. Polytech.* 23 (1), 161-169. https://doi.org/10.2339/politeknik.557592.

Bozkurt, A., Çakmakkaya, M., Çetkin, A., Talaş, Ş. (2016). Heat transfer and electrical characteristics in spot welding with composite coated caps. Proc. International Conference on Welding Technologies and Technology, (ICWET'16), Ankara.

Bozkurt, B., Emre Ertek, H., Kaçar, R. (2018). Effect of Electrodes Coated with Different Materials by Electrospark Method on the Resistance Spot Weld Quality. *Int. J. Sci. Eng. Res.* 9 (8), 81-86. https://www.ijser.org/researchpaper/Effect-of-Electrodes-Coated-with-Different-Materials-by-Electrospark-Method-on-the-Resistance-Spot-Weld-Quality.pdf.

Chen, Z., Zhou, Y. (2006). Surface modification of resistance welding electrode by electro-spark deposited composite coatings: Part I coating characterization. *Surf. Coat. Technol*. 201 (3-4), 1503–1510. https://doi.org/10.1016/j.surfcoat.2006.02.015.

Choi, H.S., Park, G.H., Lim, W.S., Kim, B.M. (2001). Evaluation of weldability for resistance spot welded single-lap joint between Ga780DP and hot-stamped 22MnB5 steel sheets. *J. Mech. Sci. Technol.* 25, 1543-1550. https://doi.org/10.1007/s12206-011-0408-x.

Demirbilek, O., Onan, M., Ünlü, N., Talaş, Ş. (2022). Investigation of the efficiency for ESD coating with stainless steel on die surfaces. *Int. J. Surf. Sci. Eng.* 16 (4), 335-348. https://doi.org/10.1504/IJSURFSE.2022.10049062.

Gould, J. (2011). Application of electro-spark deposition as a joining technology. *Weld. J.* 90 (10), 191–197.

Harlin, N., Jones, T.B., Parker, J.D. (2003). Weld growth mechanism of resistance spot welds in zinc coated steel. *J. Mater. Process. Technol.* 143-144, 448–453. https://doi.org/10.1016/S0924-0136(03)00447-3.

Holliday, R., Parker, J.D., Williams, N.T. (1995). Electrode deformation when spot welding coated steels. *Weld. World.* 35 (3), 160–164.

Judkins, R.R., Rao, U.S. (2000). Fossil energy applications of intermetallic alloys. *Intermetallics* 8 (9-11), 1347–1354. https://doi.org/10.1016/S0966-9795(00)00110-2.

Kaiser, J.G., Dunn, G.J., Eagar, T.W. (1982). The effect of electrical resistance on nugget formation during spot welding. *Weld. J.* 62 (6), 167s–174s. https://eagar.mit.edu/publications/Eagar026.pdf.

Korkmaz, K. (2015). Investigation and characterization of electrospark deposited chromium carbide-based coating on the steel. *Surf. Coat. Technol.* 272, 1–7. https://doi.org/10.1016/j.surfcoat.2015.04.033.

Korkmaz, K., Ribalko, A.V. (2011). Effect of pulse shape and energy on the surface roughness and mass transfer in the electrospark coating process. *Metallic Mater.* 49 (4), 265 – 270. https://doi.org/10.4149/km_2011_4_265.

Krein, R., Schneider, A., Sauthoff, G., Frommeyer, G. (2007). Microstructure and mechanical properties of Fe_3Al -

based alloys with strengthening boride precipitates. *Intermetallics* 15 (9), 1172–1182. https://doi.org/10.1016/j.intermet.2007.02.005.

Li, W., Cheng, S., Hu, S.J., Shriver, J. (2001). Statistical investigation on RSW quality using a two-stage, sliding-level experiment. ASME *J. Manuf. Sci. Eng.* 123 (3), 513–520. https://doi.org/10.1115/1.1382595.

Luo, Y., Wan, R., Yang, Z., Xie, X. (2016). Study on the thermo-effect of nugget growing in single-phase AC resistance spot welding based on the calculation of dynamic resistance. *Measurement* 78, 18–28. https://doi.org/10.1016/J.MEASUREMENT.2015.09.034.

Masset, P., Texier, D., Schütze, M. (2009). Coefficients of thermal expansion of (Ni0.5Al0.5) (1–x)Hfx alloys (x= 0...0.2). *Mater. Sci. Technol.* 25 (7), 874-879. https://doi.org/10.1179/174328408X372083.

Mertgenç, E., Talaş, Ş., Gökçe, B. (2019). The wear and microstructural characterization of copper surface coated with TiC reinforced FeAl intermetallic composite by ESD method. *Mater. Res. Express* 6 (11), 1165e7. https://doi.org/10.1088/2053-1591/ab507e.

Mikno, Z, Bartnik, Z. (2016). Heating of electrodes during spot resistance welding in FEM calculations. *Arch. Civ. Mech. Eng.* 16 (1), 86-100. https://doi.org/10.1016/j.acme.2015.09.005.

Morris, D.G., Munoz-Morris, M. (2005). The stress anomaly in FeAl-Fe3Al alloys. *Intermetallics* 13 (12), 1269–1274. https://doi.org/10.1016/j.intermet.2004.08.012.

Onan, M., Şahin, O., Yıldırım, E., Talaş, Ş. (2022). Effect of WC based coatings on the wear of CK45 sheet metal forming dies. *Int. J. Surf. Sci. Eng.* 15 (4), 265-280. https://doi.org/10.1504/IJSURFSE.2021.120959.

Parkansky, N., Boxman, R.L., Goldsmith, S. (1993). Development and application of pulsed-air-arc deposition. *Surf. Coat. Technol.* 61 (1-3) 268-273. https://doi.org/10.1016/0257-8972(93)90237-I.

Rogeon, P., Carre, P., Costa, J., Sibilia, G., Saindrenan, G. (2008). Characterization of electrical contact conditions in spot welding assemblies. *J. Mater. Process. Technol.* 195 (1–3), 117–124. https://doi.org/10.1016/j.jmatprotec.2007.04.127.

Schaefer, H-E., Frenner, K., Würschum, R. (1999). High temperature atomic defect properties and diffusion processes in intermetallic compounds. *Intermetallics* 7 (3-4), 277–287. https://doi.org/10.1016/S0966-9795(98)00121-6.

Song, Q., Zhang, W., Bay, N. (2005). An experimental study determines the electrical contact resistance in resistance welding. *Weld. J.* 84 (5), 73s–76s.

Stoloff, N., Liu, C., Deevi, S. (2000). Emerging applications of intermetallics. *Intermetallics* 8 (9-11), 1313–1320. https://doi.org/10.1016/S0966-9795(00)00077-7.

Švec, M., Hanus, P., Vodičková, V. (2013). The coefficient of thermal expansion of Fe_3Al and feal – type iron aluminides. *Manuf. Technol.* 13 (3), 399-404. https://doi.org/10.21062/ujep/x.2013/a/1213-2489/MT/13/3/399.

Talaş, Ş. (2018). *Nickel Aluminides*. in, *Intermetallic matrix composites*. R. Mitra (Ed.), Woodhead Publishing, pp. 37-69. https://doi.org/10.1016/B978-0-85709-346-2.00003-0.

Tang, S.K., Nguyen, T.C., Zhou, Y. (2010). Materials transfer in electro-spark deposition of TiCp/Ni metal-matrix composite coating on Cu substrate. *Weld. J.* 89 (8), 172s-180s.

Terada, Y., Ohkubo, K., Mohri, T., Suzuki, T. (2002). Thermal conductivity of intermetallic compounds with metallic bonding. *Mater. Trans.* 43 (12), 3167-3176.

Tortorelli, P., Natesan, K. (1998). Critical factors affecting the high temperature corrosion performance of iron aluminides. *Mater. Sci. Eng. A* 258 (1-2), 115–125. https://doi.org/10.1016/S0921-5093(98)00924-1.

Wan, X., Wang, Y., Zhang, P. (2014). Modelling the effect of welding current on RSW of DP600 steel. *J. Mater. Process. Technol.* 214 (11), 2723–2729. https://doi.org/10.1016/j.jmatprotec.2014.06.009.

Wang, K., Reeber, R.R. (1996). Thermal expansion of copper. *High Temp. Mater. Sci.* 35, 181-186.

Wang, Y., Liu, Z-K., Chen, L-Q. (2004). Thermodynamic properties of Al, Ni, NiAl, and Ni3Al from first-principles calculations. *Acta Mater.* 52 (9), 2665–2671. https://doi.org/10.1016/j.actamat.2004.02.014.

Williams, N.T., Parker, J.D. (2004). Review of resistance spot welding of steel sheets Part 1: modelling and control of weld nugget formation. *Int. Mater. Rev.* 49 (2), 45–75. https://doi.org/10.1179/095066004225010523.

Zhang, X.Q., Chen, G.L., Zhang, Y.S. (2008). Characteristics of electrode wear in RSW dual-phase steels. *Mater. Des.* 29 (1), 279-283. https://doi.org/10.1016/j.matdes.2006.10.025.